SUPPORTING INFORMATION

Size, Shape, Facet and Support Dependent Selectivity of Cu nanoparticles in CO_2 reduction through multiparameter optimization

Anjana Tripathi[a], Ranjit Thapa[a,b] *

[a]Department of Physics, SRM University AP, Amaravati 522 240 Andhra Pradesh, India

[a,b]Centre for Computational and Integrative Sciences, SRM University – AP, Amaravati 522 240, Andhra Pradesh, India

*Corresponding Author: ranjit.phy@gmail.com

S.No.	Surface	G_{*COOH}	G_{*CO}	G_{*CHO}	G(C1) (G_{*CHO}-G_{*CO})	G(C2) (G_{*2CO})-(G_{*COCOH})	Favorable pathway
1	Cu111	0.38	-0.04	0.63	0.67	0.73	C1
2	Cu100	0.35	-0.05	0.60	0.65	0.49	C2
3	Cu13	0.09	-0.39	0.29	0.68	0.74	C1
4	Cu38(100)	0.22	0.45	0.51	0.06	0.77	C1
5	Cu38(111)	0.50	0.01	0.63	0.62	0.51	C2
6	Cu55(100)	0.22	-0.09	0.44	0.53	0.42	C2
7	Cu55(111)	0.15	-0.02	0.39	0.41	0.68	C1
8	Cu79(100)	-0.32	-0.54	0.17	0.71	0.55	C2
9	Cu79(111)	0.01	-0.38	0.31	0.69	0.59	C2
10	Cu140(100)	-0.40	-0.75	-0.10	0.65	0.66	C1
11	Cu140(111)	-0.11	-0.37	0.13	0.5	0.69	C1
12	Cu147(100)	-0.16	0.15	0.11	-0.04	0.51	C1
13	Cu147(111)	-0.37	0.13	0.66	0.53	0.62	C1
14	Cu13(Ico)	-0.83	-0.68	-0.56	0.12	1.2	C1
15	Cu55(Ico)	0.38	-0.04	0.58	0.62	0.86	C1
16	Cu147(Ico)	0.31	0.05	0.56	0.51	0.83	C1
17	Cu_{38}/3BGr	0.43	0.25	0.78	0.53	0.64	C1
18	Cu_{79}/BGr	0.33	-0.01	0.55	0.56	0.97	C1
19	Cu_{38}/DVG	0.48	0.35	0.50	0.15	0.22	C1
20	Cu_{79}/DVG	0.33	-0.03	0.23	0.26	1.08	C1
21	Cu_{55}/DVG	0.33	-0.07	0.64	0.71	0.90	C1
22	Cu_{79}/BDVG	0.47	0.01	0.32	0.31	1.10	C1
23	Cu_{147}/BDVG	0.33	0.11	0.66	0.55	0.71	C1
24	Cu_{55}/NDVG	0.28	-0.07	0.53	0.60	0.62	C1
25	Cu_{55}/2NDVG	-3.43	-0.08	-3.05	-2.97	-2.72	C2
26	Cu_{147}/2NDVG	0.26	0.11	0.63	0.52	0.66	C1
27	Cu38/2SO$_2$	0.46	0.40	0.78	0.38	0.18	C2
28	Cu55/2SO$_2$	-3.76	-0.14	0.46	0.60	0.71	C1
29	Cu79/2SO$_2$	0.44	0.11	0.65	0.54	0.49	C2
30	Cu140/2SO$_2$	0.53	0.25	0.75	0.50	0.58	C1

Table S1. Gibbs free energy (ΔG_{*COOH}, ΔG_{*CO}, ΔG_{*CHO}) of first four PCET steps in reaction pathway of CO_2RR along with the barrier for C1 and C2 pathway on the systems considered in this work. All units are in eV.
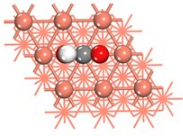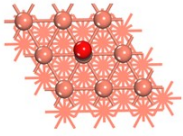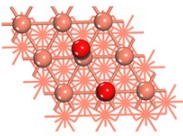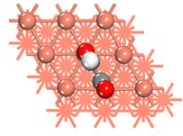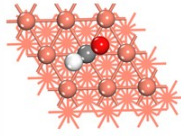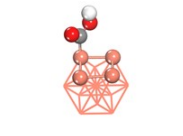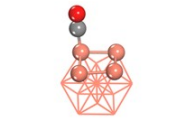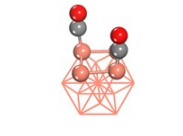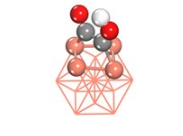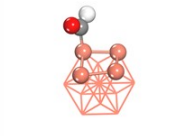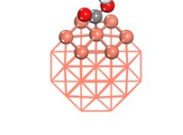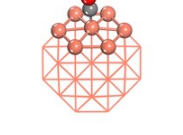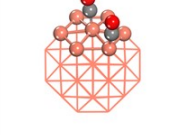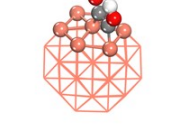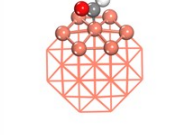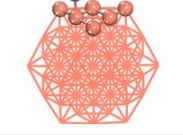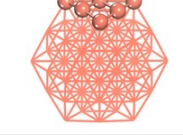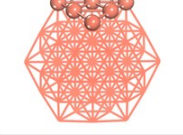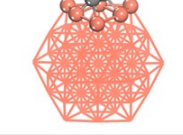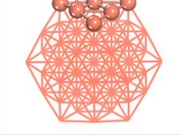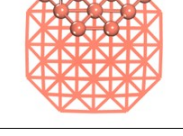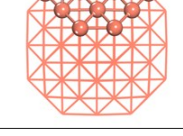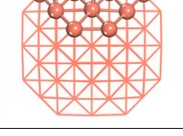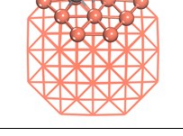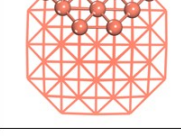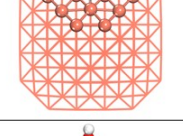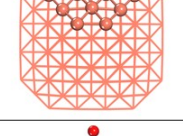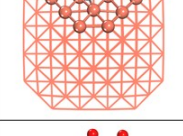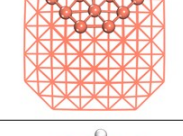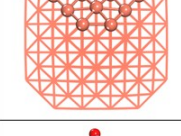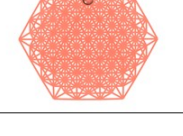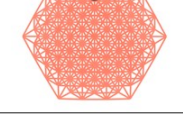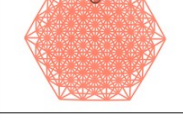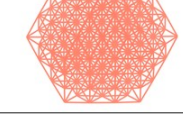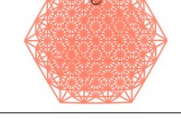
Metal	*COOH	*CO	*2CO	*COCOH	*CHO
Cu(111)					
Cu_{13}					
Cu_{38}					
Cu_{55}					
Cu_{79}					
Cu_{140}					
Cu_{147}					

Fig. S1 Optimized geometries of key intermediates adsorbed on the Cu (111) plane and Cu_n (n = 13, 38, 55, 79, 140 and 147) clusters and the extended surfaces.
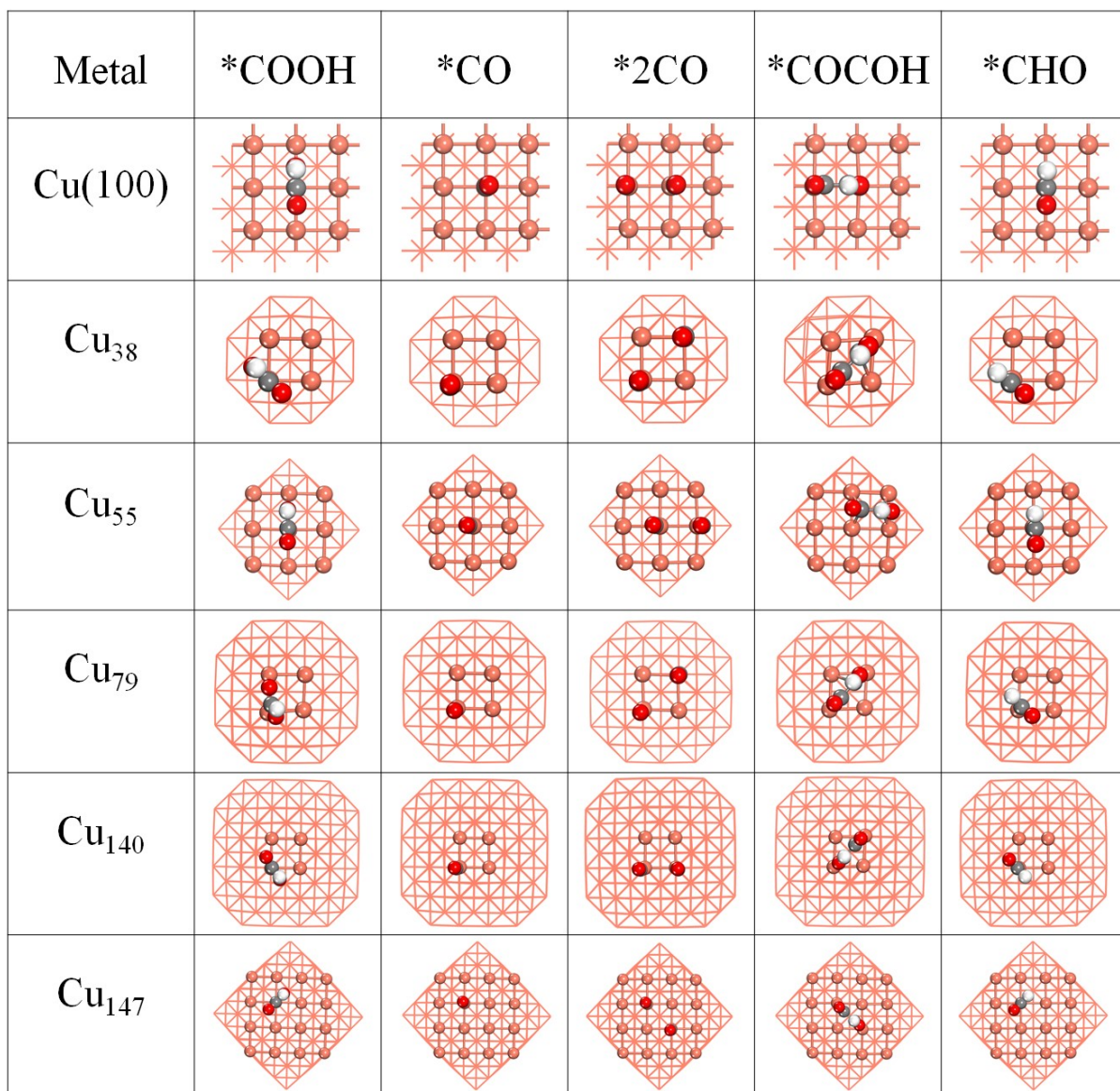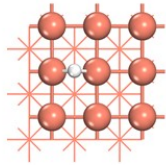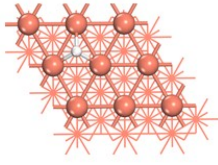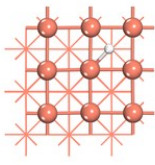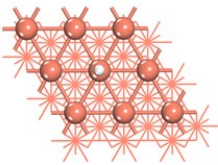
Metal	*COOH	*CO	*2CO	*COCOH	*CHO
Cu(100)					
Cu$_{38}$					
Cu$_{55}$					
Cu$_{79}$					
Cu$_{140}$					
Cu$_{147}$					

Fig. S2 Optimized geometries of key intermediates adsorbed on the Cu (100) plane and Cun (n = 13, 38, 55, 79, 140 and 147) clusters and the extended surfaces.
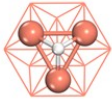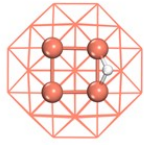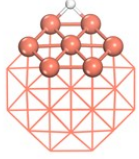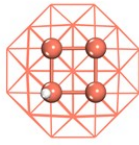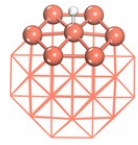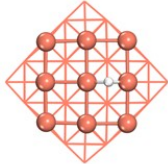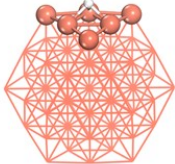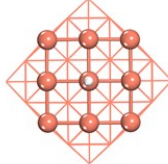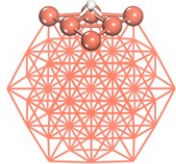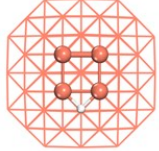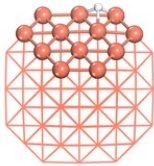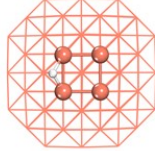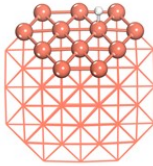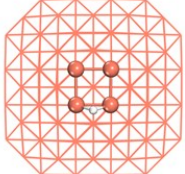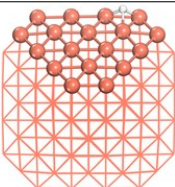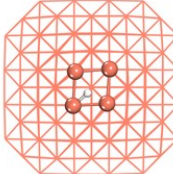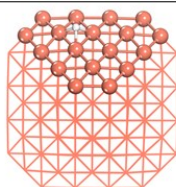
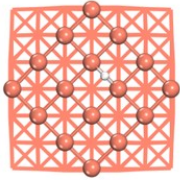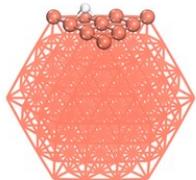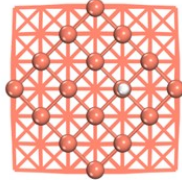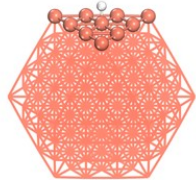| Metal	*H@(100)	*H@(111)	*H@(100) Top site	*H@(100) Top site
Cu-plane				
Cu_{13}		--	--	--
Cu_{38}				
Cu_{55}				
Cu_{79}				
Cu_{140}				
Cu_{147}				

Fig. S3 Optimized geometries of hydrogen atom adsorption on the bridge site and atop site of 100 and 111 plane of Copper nanoparticles.

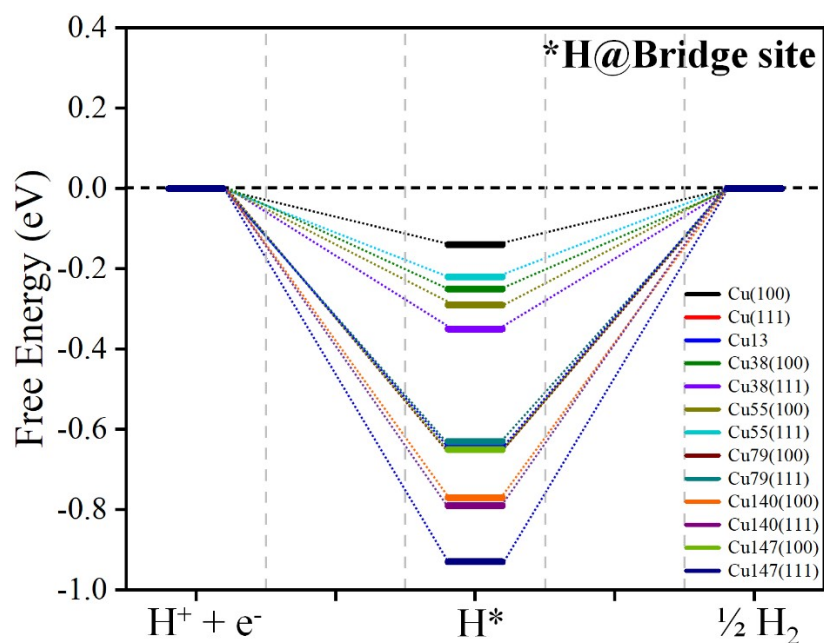**Fig. S4** Free energy diagram of Hydrogen evolution reaction on bridge site of nanoparticle having different size and shape (see Figure S3 for sites and model structure). Units are in eV.
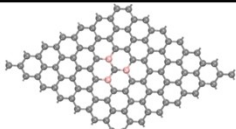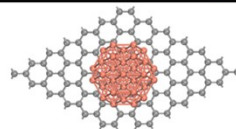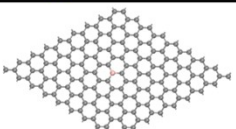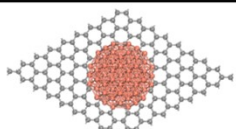

Fig. S5 Optimized structures of Copper nanoparticle (in blue color) anchored on host surface (in black color).
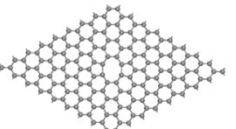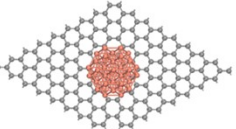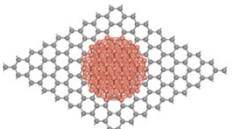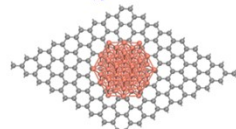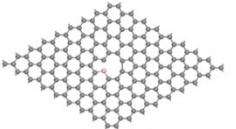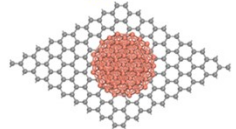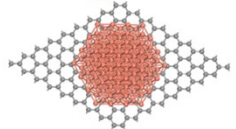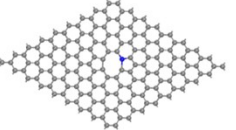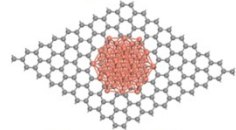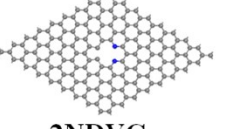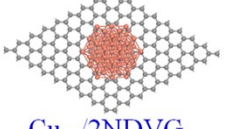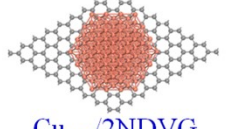
Host Surface	Nanoparticle Supported on Host Surface	
2SO₂-ZGNR **Side view:** **Top view:**	Cu₃₈/2SO₂	Cu₅₅/2SO₂
	Cu₇₉/2SO₂	Cu₁₄₀/2SO₂

Fig. S6 Optimized structures of Copper nanoparticle (in blue color) anchored on host surface (in black color) edge doped $2SO_2$ graphene nanoribbon.

Fig. S7 Free energy profiles (ΔG) of reaction pathway of CO_2RR with the first four PCET steps and C-C coupling process (a). On 111 facet of Cu_{38} and Cu_{79} supported on heteroatom doped graphene (b). On 111 facet of Cu_{55} and Cu_{147} supported on heteroatom doped graphene.

Fig. S8 Free energy profiles (ΔG) of reaction pathway of CO_2RR to C_2H_4 with *2CO-*COCOH formation pathway on 111 facet of three selected nanoparticles ($Cu_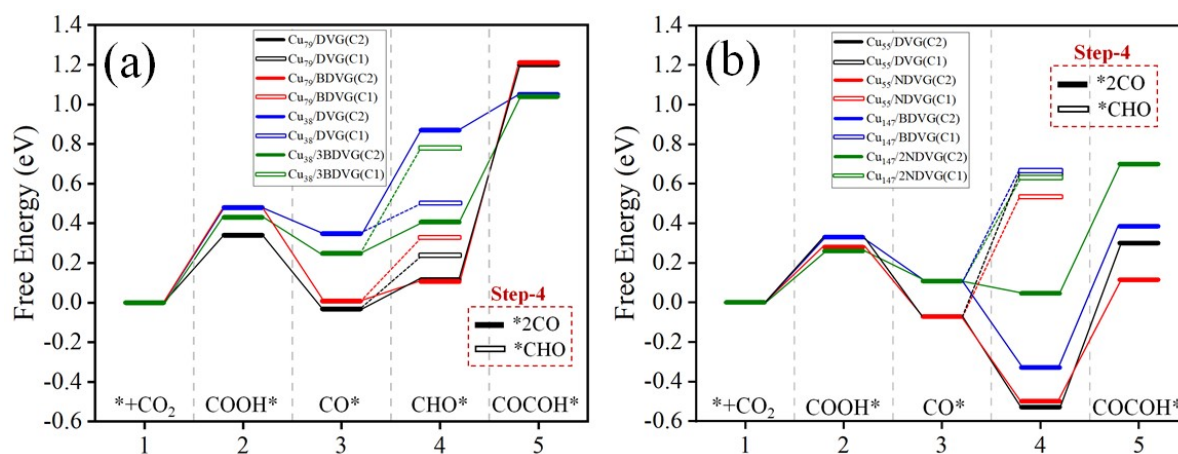{38}$, Cu_{79}, Cu_{140}) and extended surface (2SO_2 doped graphene nanoribbon) (Cu_{38}/SO_2, Cu_{79}/SO_2).

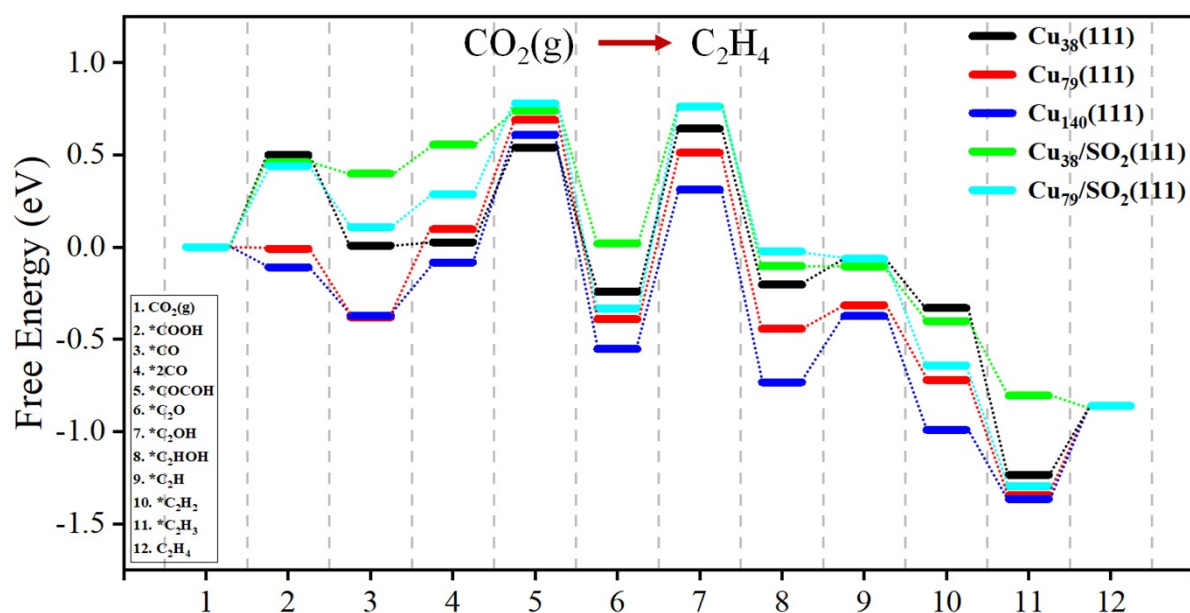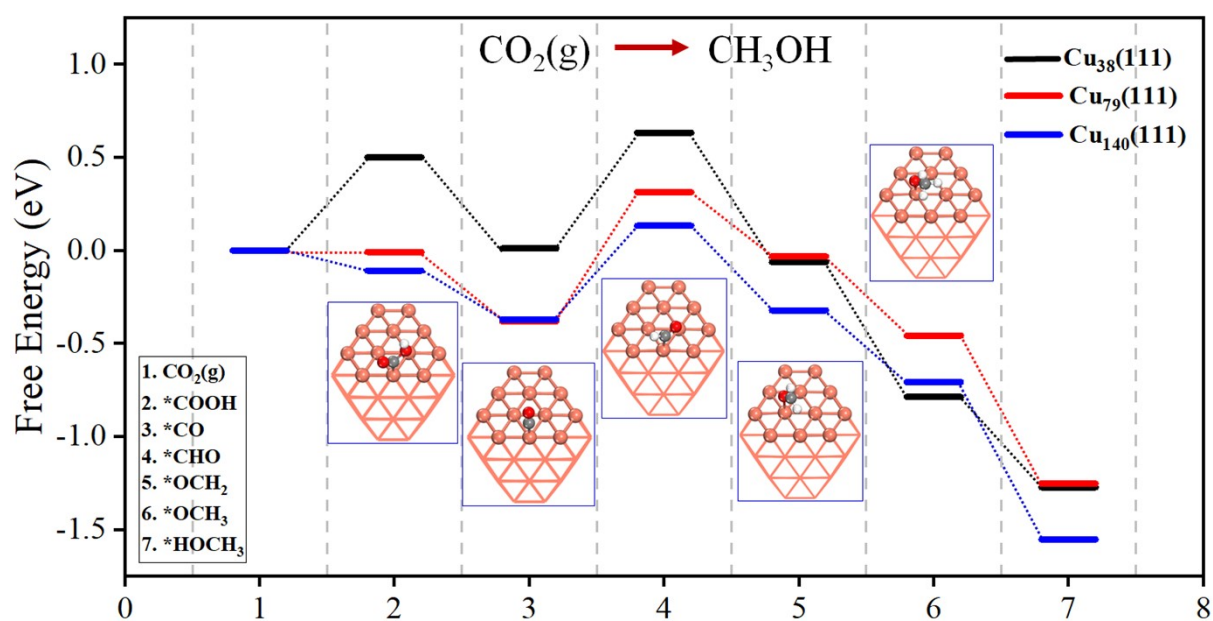**Fig. S9** Free energy profiles (ΔG) of reaction pathway of CO_2RR to CH_3OH with *CO-*CHO formation pathway on 111 facet of three selected nanoparticles (Cu_{38}, Cu_{79}, Cu_{140}). An illustrative example of Cu_{79} of intermediate structures is shown in the inset.
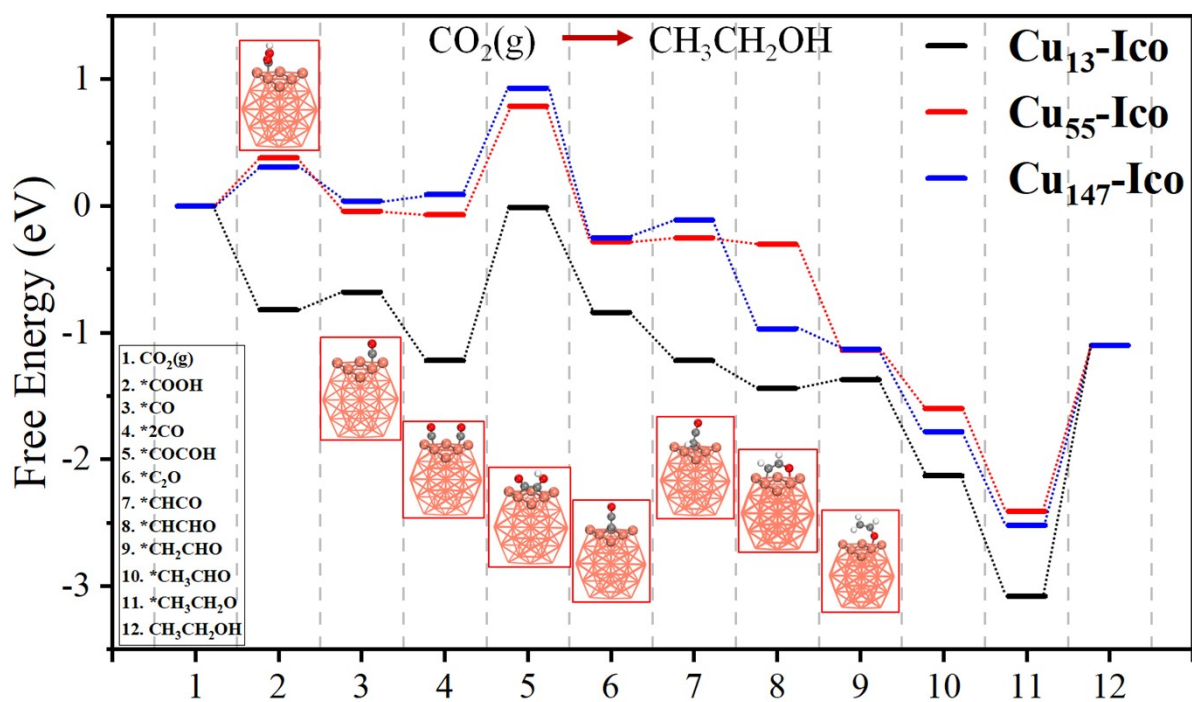
Fig. S10 Free energy profiles (ΔG) of reaction pathway of CO_2RR to C_2H_5OH with *2CO-*COCOH formation pathway on 111 facet of Icosahedral nanoparticles (Cu_{13}, Cu_{55}, Cu_{147}). An illustrative example of Cu_{55} of intermediate structures is shown in the inset.
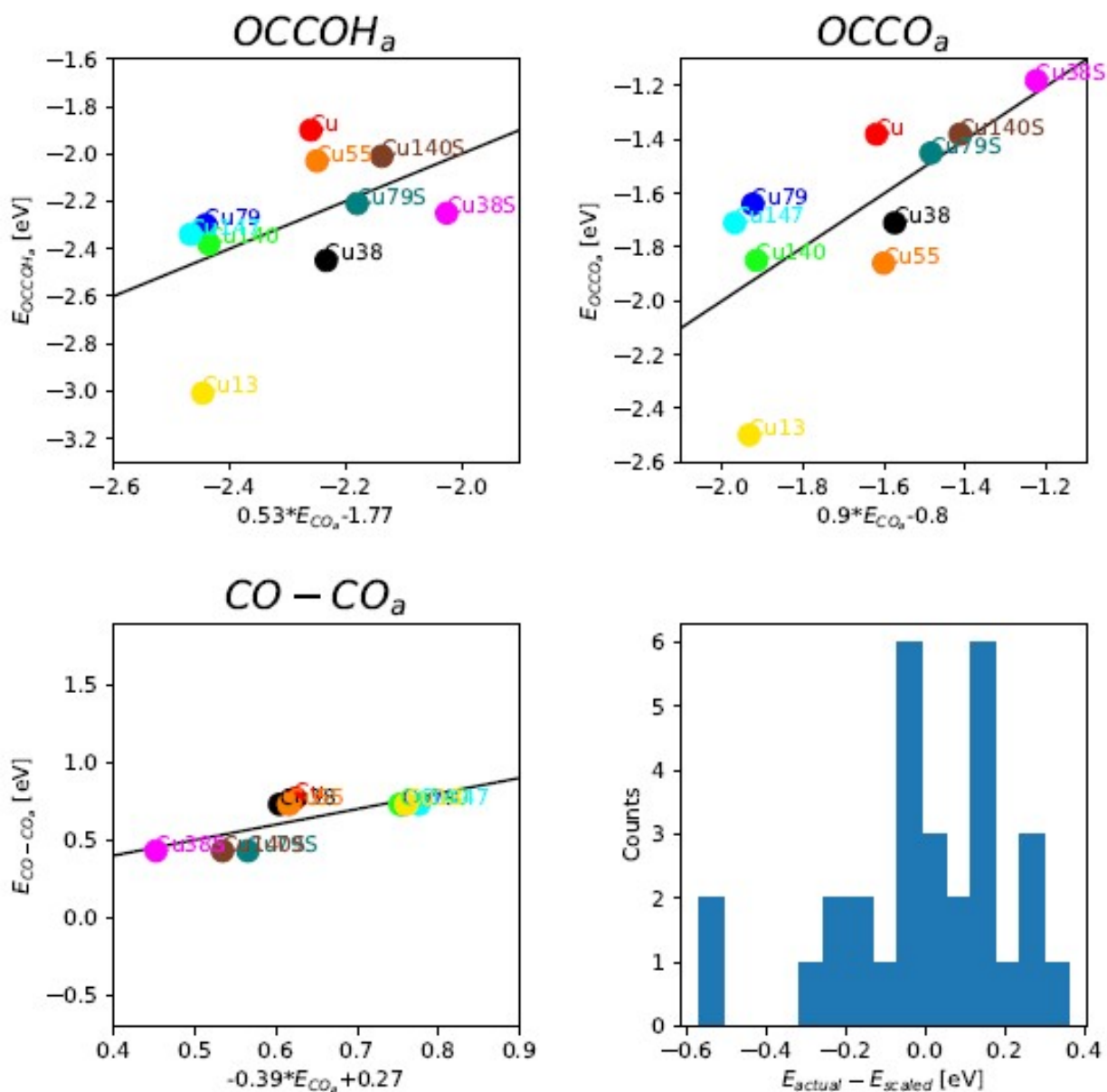
Fig. S11 Scaling relations on the (111) surface of Cu nanoparticles between the binding energies of the intermediates versus the binding energies of the descriptors *CO.
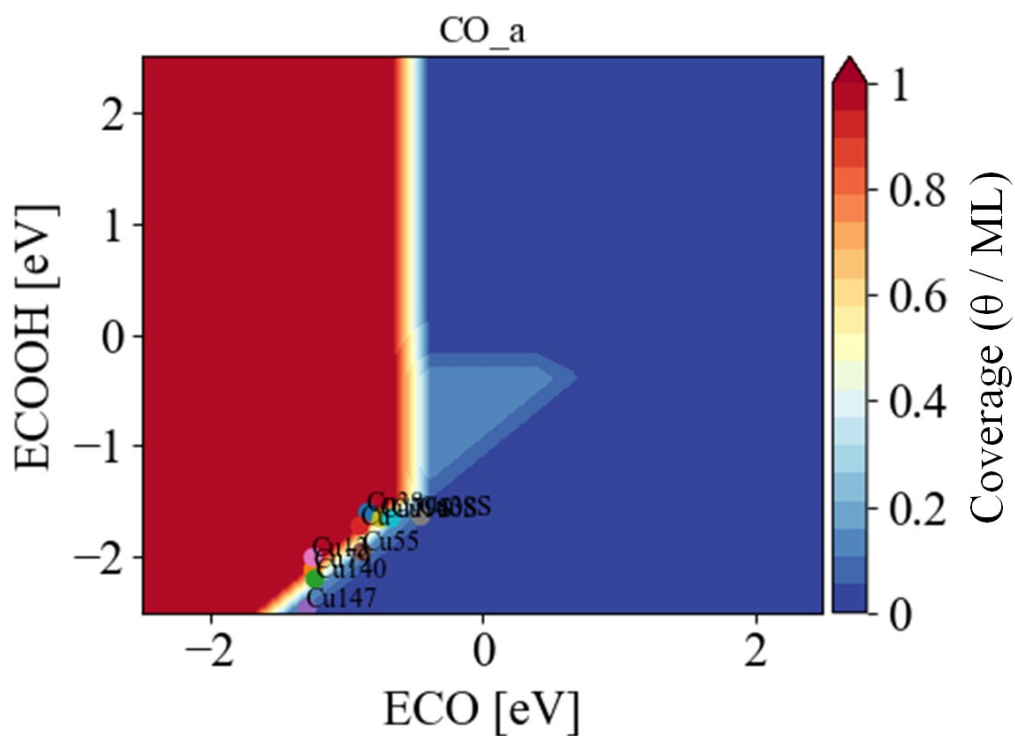
Fig. S12 CO coverage map for Cu nanoparticles obtained using microkinetic model based on scaling relations.
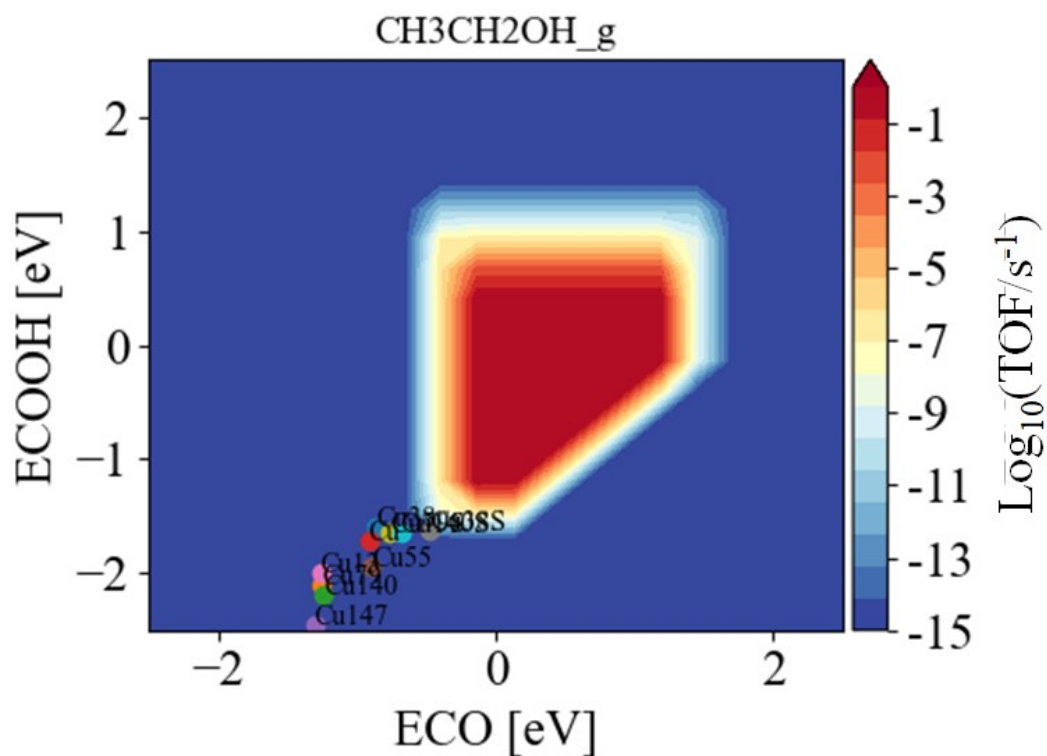

Fig. S13 Activity volcano plot for Cu nanoparticles plotted using the binding energy of *CO and *COOH intermediate as the activity descriptors.